The Molecular Orientation and Mechanical Properties of Poly(ethylene Terephthalate) Under Uniaxial Extension

C. L. CHANG,[1] W. Y. CHIU,*[1], K. H. HSIEH,[1] and C.-C. M. MA[2]

[1]Department of Chemical Engineering, National Taiwan University, Taipei, Taiwan, Republic of China; and
[2]Department of Chemical Engineering, National Tsung Hua University, Hsin-Chu, Taiwan, Republic of China

SYNOPSIS

The molecular orientation, induced crystallization, and mechanical properties of amorphous poly(ethylene terephthalate) (PET), stretched at different temperatures and strain rates, were studied. The results indicate that the orientation parameter $[P_2(\cos\theta)]$ of oriented PET varies strongly with both temperature and strain rate, but the strain-induced crystallinity seems dependent on temperature only. It was also found that as draw ratio increased, the Young's modulus, yield stress, and necking ratio were greatly improved in the stretching direction, but slightly declined in the transverse direction. A rubber network model was used to make a quantitative description of the orientation development with draw ratio.

INTRODUCTION

Many studies[1-14] have been performed on the development of molecular orientation, induced crystallization, and mechanical behaviors in poly(ethylene terephthalate) (PET) under extension, because of the importance of PET in the manufacture of fibers and films. It is reported that these three properties are closely related with one another when amorphous PET is stretched between its glass transition temperature (T_g) and normal crystallization temperature (T_c). Generally, these properties and their relationships are strongly influenced by the draw ratio (λ), temperature (T), and strain rate ($\dot{e}$).[4] When the polymer is stretched, their molecular chains become aligned with the draw direction by its entanglement with neighboring chains. Between T_g and T_c, the thermal relaxation rate of molecular chains competes in opposition to strain rates applied to the polymer. Molecular orientation and strain-induced crystallization can be generated and further increased only when the rate of strain surpasses the thermal relaxation rate.

A variety of methods, based on optical birefringence,[8,9,11] spectroscopy,[2,11,13] fluorescence,[11,14] X-ray scattering,[2,3,8,11] and light scattering,[6,8] have been used to investigate the structural development of extended PET. Ward and coworkers[5,11,12,14] made use of various structural techniques to measure the degree of the molecular alignments of stretched PET and found that the values of the orientation parameter $[P_2(\cos\theta)]$ from different methods were fairly consistent. To quantitatively describe the orientation development with draw ratio above T_g, the rubber network model of Roe and Krigbaum[15] was widely used,[8,11,13] especially for the low $[P_2(\cos\theta)]$ values. Nobbs et al.[16,17] later modified this model and got fairly good agreement with experimental results up to high draw ratio. A number of investigations have been performed on the strain-induced crystallization during stretching of PET. It is known[18] that the mechanism of crystallization changes from a three dimensional spherulite shape to a one dimensional fibrillar structure as the orientation increases. In addition, the entropic reduction during extension was proposed[19] to be related to the origin of induced crystallization. LeBourvellec and coworkers[20] systematically investigated the strain-induced crystallization during the stretching of PET above T_g. They found the crystallinity induced is dependent clearly on temperature but not

* To whom correspondence should be addressed.

Journal of Applied Polymer Science, Vol. 50, 855–862 (1993)
 CCC 0021-8995/93/050855-08

so much on strain rate. On the part of mechanical properties, extensive studies[7,9,10,21,22] have been undertaken. It was found that the anisotropy of the mechanical properties of stretched PET was strongly influenced by the molecular orientation and crystallinity. A number of models, such as the aggregate model[10] and the composite model,[10,22] have been proposed to correlate the orientation and morphology of stretched PET with its mechanical behaviors.

The present work reports on the development of molecular orientation and induced crystallization of isotropic amorphous PET at different constant strain rates and temperatures between T_g and T_c. The modified rubber network model, originally proposed by Nobbs and Bower,[13,16,17] is used as the deformation mechanism to explain phenomenally the variation of the orientation parameter $[P_2(\cos\theta)]$ as a function of draw ratio. The Young's modulus and yield stress of a series of extended PET samples were also measured to investigate the effect of molecular orientation on the mechanical properties of oriented PET.

EXPERIMENTAL

Specimen Preparation

The starting material is crystallized PET granules with an intrinsic viscosity of 0.5, which were kindly supplied by Far-East Textile Company, Shinju, Taiwan. Before use, the starting material is always dried for 24 h in an oven at constant temperature 130°C. The procedure of specimen preparation is as follows: First, the stainless mold with inner size 12 cm/12 cm/0.06 cm was fully loaded with dried granules and was covered on both sides with aluminum sheets, and was then hot-pressed at 280°C for 5 min. After PET fully melted, the mold was quickly quenched by placing it in ice water for about 20 min. Finally, the polymer plates were taken out of mold and kept in 80°C for 6 h to eliminate internal stress. Examination by the wide angle X-ray method showed the prepared plates to be amorphous and unoriented.

Prepared amorphous PET plates were cut into 6 cm/5 cm/0.06 cm small plates. The direction with the length of 6 cm was chosen as the stretching direction. Perpendicular to that direction, a series of straight parallel lines with 2 mm spacing were drawn on the plates. The extension of the specimen was performed in a hot-air oven by an Instron tensile testing machine (RTM-1T, Orientec) under constant temperatures and strain rates. Before stretching started, the plate was warmed up to the operation temperature by holding it with two Instron clamps, 5 cm apart from each other, in the oven for 5 min. After attaining the extension length, the stretched plate was cooled quickly by contact with ice-cold steel plates in order to freeze its morphology and orientation. The draw ratio can be calculated from the distance of the originally marked lines. In this study, operation temperatures ranged from 70°C to 100°C and strain rates were from 0.000333 s^{-1} to 0.166667 s^{-1}.

Finally, the central portions of the stretched plates, with uniform draw ratio, were tailored into smaller samples for different characterizations.

Molecular Orientation Determination

From the measurements of the refractive indices of the samples for light polarized with the electric vector parallel to draw direction, n_z, and normal to this direction, n_x, the second order orientation parameter $[P_2(\cos\theta)]$, defined as $\frac{1}{2}[3(\cos^2\theta) - 1]$ was obtained by using the relationship[12]:

$$\frac{\phi_z^e - \phi_x^e}{\phi_z^e + 2\phi_x^e} = \frac{\Delta\alpha}{3\alpha_0}[P_2(\cos\theta)] \tag{1}$$

where $\phi_i^e = (n_i^2 - 1)/(n_i^2 + 2)$, $i = x, z$. $\Delta\alpha$ is the difference between the electronic polarizabilities of a polymer structural unit parallel and perpendicular to the chain axis, and α_0 is the isotropic polarizability. The value $\Delta\alpha/3\alpha_0$ can be measured from the highly oriented PET. However, instead of measuring in this experiment, the value 0.105 was adopted from the paper of Cunningham and coworkers.[12]

An Abbe refractometer (3T, Atago), with monochromatic light (wavelength 589 nm), was used to measure the refractive indices n_x and n_z by placing the oriented plates along stretching and transverse directions. Chemicals with a high refractive index, α-Bromonaphthalene ($n = 1.65$) and methylene iodide ($n = 1.74$), were used. In order to enhance the resolution, two additional polarized filters were used with the refractometer.

Crystallinity Determination

The crystallinity X (volume percent) is calculated from the density of polymer samples by the following equation:

$$X = \frac{\rho_c - \rho}{\rho_c - \rho_a} \tag{2}$$

The density of amorphous phase ρ_a is taken to be 1.335 g/cm^3 and that of crystalline phase ρ_c as 1.455 g/cm.[3,8]

The density of stretched plates (ρ) was measured by the pycometric method using the following equation:

$$\rho = \frac{\rho_W W_1}{W_0 + W_1 - W_2} \tag{3}$$

where ρ_W = density of water (1 g/cm^3), W_0 = weight of pycometer filled with water, W_1 = sample weight, and W_2 = weight of pycometer with sample and water. Approximately 1 gram of polymer sample was used in each measurement and the accuracy is about 0.002 g/cm^3.

Young's Modulus and Yield Stress Measurement

The stretched plates, for which orientation had been measured, were cut into dumbell shape and were drawn in the Instron tensile testing machine at room temperature. This tensile test is according to the ASTM D638 method with a constant strain rate 0.01667 s^{-1}. Young's modulus and yield stress were then calculated from recorded load–elongation curve.

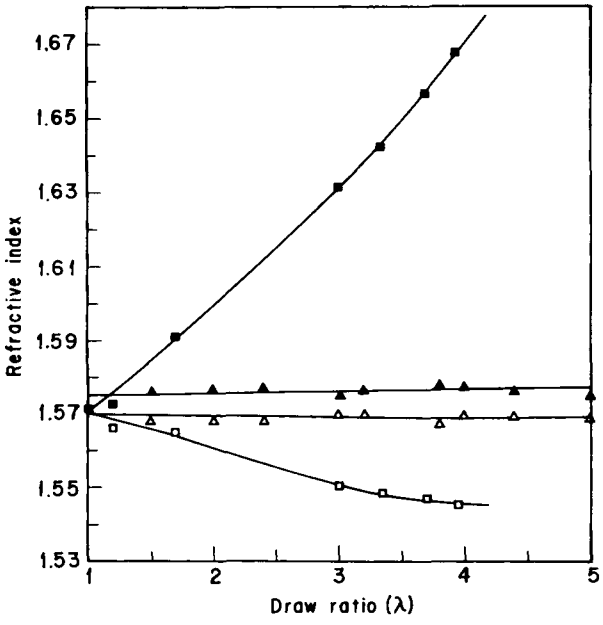

Figure 1 The refractive index vs. draw ratio. At 70°C and 0.00033 s^{-1}: (■) n_z, (□) n_x; at 100°C and 0.1667 s^{-1}: (▲) n_z, (△) n_x.

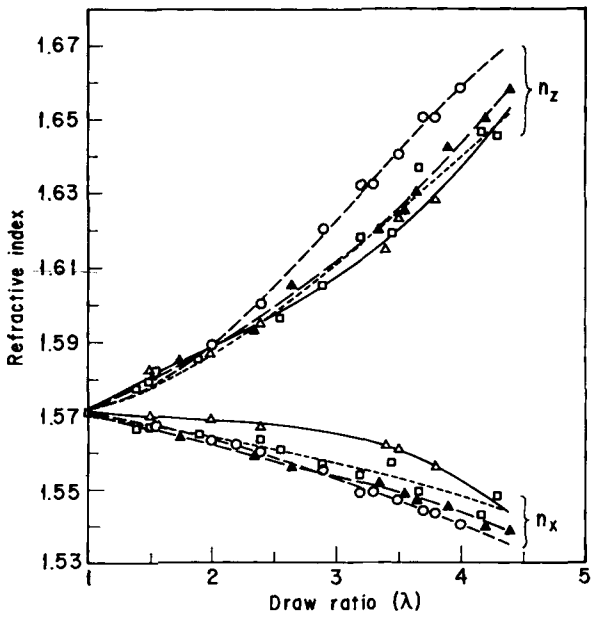

Figure 2 The refractive index (n_z and n_x) vs. draw ratio at 80°C. (△) 0.001 s^{-1}, (□) 0.0033 s^{-1}, (▲) 0.01 s^{-1}, (○) 0.033 s^{-1}.

RESULTS AND DISCUSSION

Molecular Orientation

Four temperatures, between T_g and T_c, were selected for the stretching of the PET specimen. They were 70°C, 80°C, 90°C, and 100°C. We found that temperature had a significant effect on the chain mobilities, and the strain rates were adjusted for different operation temperatures. At 70°C (glass-transition region), a very low strain rate is required for PET to be stretched to high draw ratio without the occurrence of necking, and we used the rate 0.00033 s^{-1} to obtain highly oriented samples. At 100°C (liquid-flow region), even under the highest strain rate, 0.16667 s^{-1}, that the Instron machine could reach, there was still no significant orientation generated. The measurement of the refractive indices, n_x, n_z, at these two temperatures and strain rates are shown in Figure 1. At 80°C (rubber-pseudoplateau region), four different strain rates were used, and the values of measured refractive indices were plotted in Figure 2.

The refractive index of unoriented amorphous PET was measured at 1.571. The refractive index, n_z, along the stretching direction, increased with draw ratio and could rise up to 1.665 at 70°C with $\dot{e}$ = 0.00033 s^{-1}. The value n_x, perpendicular to the stretching direction, however, decreased slowly with draw ratio and could reach around 1.54.

We substituted the value of refractive indices into eq. (1) and calculated the second order orientation parameter $[P_2(\cos\theta)]$ of each sample. These values are labeled in Figures 3 and 4. Figure 3 shows the induced orientation at two temperatures: 70°C and 100°C. Figure 3 illustrates how temperature affects the relaxation rate of the PET molecular chains. At 70°C, $[P_2(\cos\theta)]$ steadily increases up to 0.57 at draw ratio 3.9 under very low strain rate. However, at 100°C and high strain rate, $[P_2(\cos\theta)]$ always stays around 0.04 without significant change, which implies thermal relaxation rates of chains are faster than the strain rate. Figure 4 shows that at 80°C, the orientation steadily increased with draw ratio under these four strain rates. Though the effects of strain rate on the rate of the $[P_2(\cos\theta)]$ increment with draw ratio do not look obvious, it is apparent that the orientations at higher strain rates are generally higher. For example, at a draw ratio equal to 3.8, $[P_2(\cos\theta)]$ is 0.31 at $\dot{e} = 0.001\ s^{-1}$, but becomes 0.47 at $\dot{e} = 0.033\ s^{-1}$.

It is of interest to find a model to describe the trend of orientation increment with draw ratio under different strain rates and temperatures. During the deformation of noncrosslinked polymer, the displacement of a molecular chain is entangled with its neighboring chains by knots and other ways. The rubber network model[15] describes this mechanism as the deformation of a crosslinked network of the chains with N statistical segments. The number N is a parameter,[23] which depends on the number of knots and entanglements between chains. Nobbs

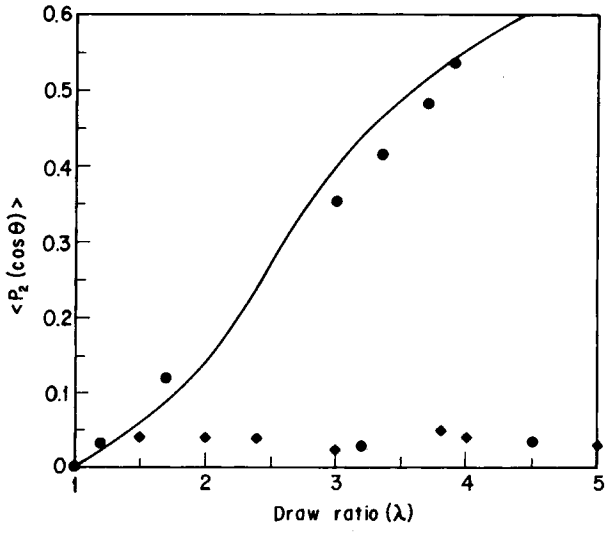

Figure 3 $[P_2(\cos\theta)]$ vs. draw ratio. (●) at 70°C, 0.00033 s^{-1}; (——) fitting through all draw ratios, N = 6; (♦) at 100°C, 0.1667 s^{-1}.

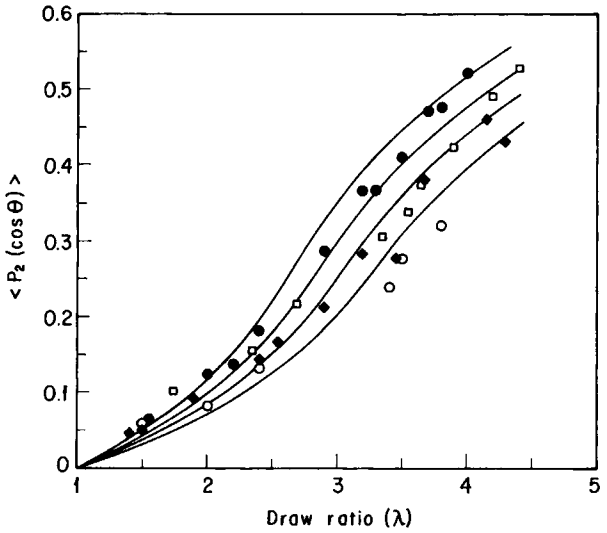

Figure 4 $[P_2(\cos\theta)]$ vs. draw ratio at 80°C. (○) 0.001 s^{-1}, (♦) 0.0033 s^{-1}, (□) 0.01 s^{-1}, (●) 0.033 s^{-1}, (——) fitting through all draw ratios, N = 11, 9.6, 8.4, and 7, respectively.

and Bower[17] found that this model is not applicable when λ approaches $(N)^{1/2}$ and they modified the model. The relations of $[P_2(\cos\theta)]$ to draw ratio (λ) were proposed by Nobbs and Bower[17]:

$$[P_2(\cos\theta)] = \frac{1}{5N}\left(\lambda^2 - \frac{1}{\lambda}\right) + \frac{1}{25N^2}\left(\lambda^4 + \frac{\lambda}{3} - \frac{4}{3\lambda^2}\right) + \frac{1}{35N^3}\left(\lambda^6 + \frac{3\lambda^3}{5} - \frac{8}{5\lambda^3}\right) \quad \text{for } \lambda^2 < N \quad (4a)$$

$$[P_2(\cos\theta)] = 1 - \frac{128N^{0.5}}{175\lambda} \quad \text{for } \lambda^2 > N \quad (4b)$$

where N is the adjustable parameter.

We used the above expressions to fit the experimental $[P_2(\cos\theta)]$ values for the whole range of draw ratio by changing the parameter N, and the results were shown as the curves in Figures 3 and 4. At 70°C and at strain rate 0.00033 s^{-1}, data can be fit well by the curve $N = 6$. At 80°C, data are in the range between curves of $N = 7$ and $N = 12$, and N = 11, 9.6, 8.4, and 7 could represent the trends of $[P_2(\cos\theta)]$ at $\dot{e}$ = 0.001, 0.0033, 0.01, and 0.0333 s^{-1}, respectively.

These calculations are shown as solid curves in Figures 3 and 4.

Crystallinity

To study the effects of temperature and strain rate on the crystallinity induced, we measured the density of a series of PET plates extended to various draw ratios at 80°C with different strain rates. Figure 5 illustrates the values of induced crystallinity as a function of draw ratio at different conditions. The initial density of the unoriented amorphous PET specimen was about 1.338–1.339 g/cm^3, which is equivalent to 3% crystallinity. At 80°C, the PET crystallizes at draw ratio greater than about 2. The start of crystallization shifts successively toward higher draw ratio when the strain rate decreases. These results are similar to those found by Le-Bourvellec and coworkers,[20] even though they determined the density of PET using a different equation, which is $\rho = 4.017\ (n^2 - 1)/(n^2 + 2)$, where n is the average refractive index of the sample.

If we plotted crystallinity as a function of orientation in Figure 6, within the limit of experimental error, the effects of strain rates could not be clearly observed. Similar results have been reported[7,20] and it is proposed that this lack of the dependency of crystallinity on strain rates is caused by the competition of two effects: the time of crystallization and the rate of crystallization.

The dashed line in Figure 6 is the linear fitting of the data at 80°C. Its slope represents the value of $\{dX/d[P_2(\cos\theta)]\}_T$. It is 0.38 at 80°C. Le-Bourvellec et al.[24] found similar values, but they made use of the fluorescence technique instead of the refractive index to measure $[P_2(\cos\theta)]$.

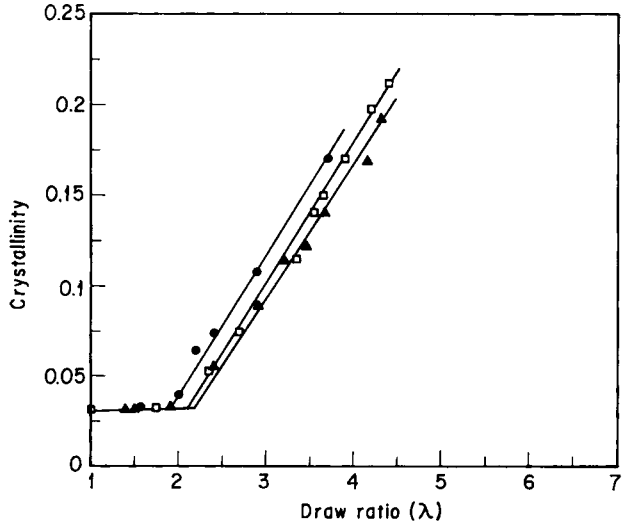

Figure 5 The crystallinity from density measurement vs. draw ratio. At 80°C: (▲) 0.0033 s^{-1}, (□) 0.01 s^{-1}, (●) 0.033 s^{-1}.

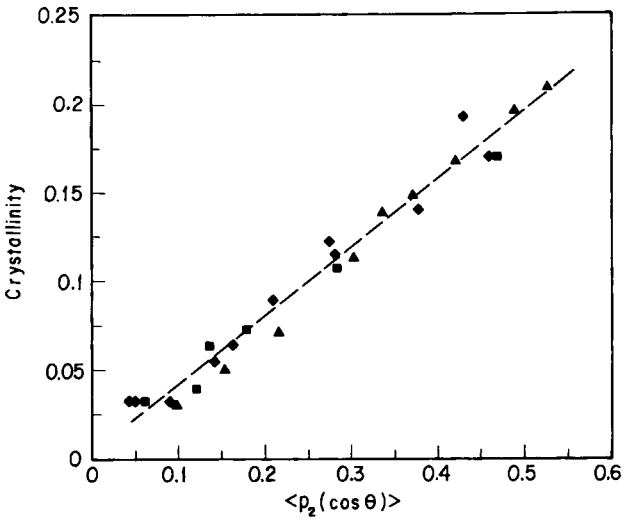

Figure 6 The crystallinity from eq. (3) vs. $[P_2(\cos\theta)]$. At 80°C: (♦) 0.0033 s^{-1}, (▲) 0.01 s^{-1}, (■) 0.033 s^{-1}, (----) linear fitting with slope 0.38.

Mechanical Properties

The load–elongation curves, shown in Figure 7, represent the general results of our tensile test of oriented PET samples at room temperature, which is about 25°C. The Young's modulus and yield stress were measured. In addition, we also used the ratio of the stresses right after and before the occurrence of necking as a representation of the extent of necking. In short, this stress ratio is defined as C/Y with C and Y illustrated in Figure 10.

Young's Modulus

Figure 8 shows Young's modulus along the stretching direction (E_z) as a function of draw ratio under dif-

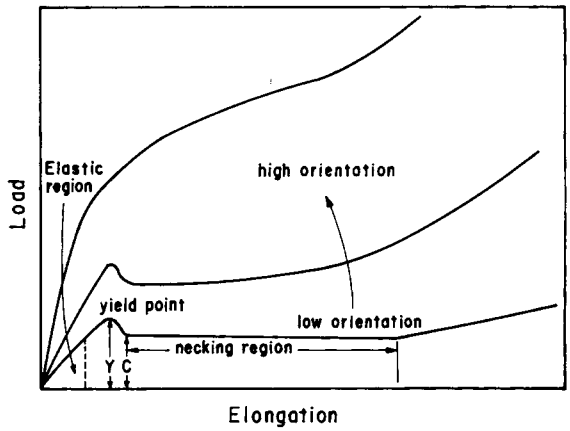

Figure 7 The load–elongation curves of oriented polymer in the stretching direction.

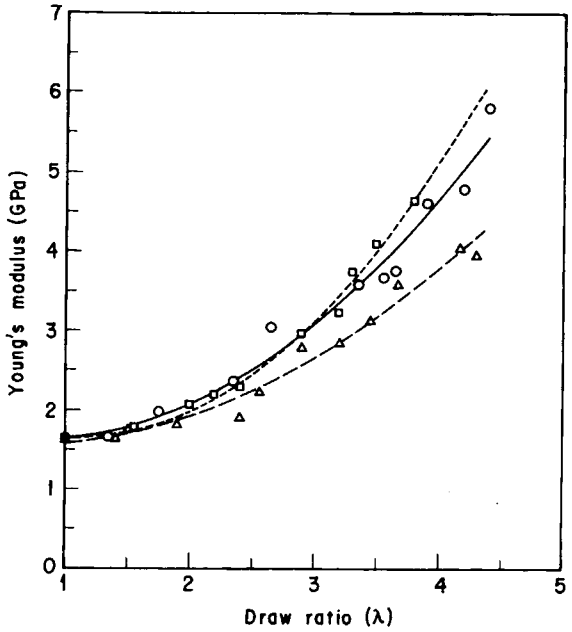

Figure 8 The Young's modulus (E_z) vs. draw ratio at 80°C. (△) 0.0033 s^{-1}, (○) 0.01 s^{-1}, (□) 0.033 s^{-1}.

ferent strain rates at 80°C. Young's modulus, E_z, rises steadily from 1.65 GPa up to about 5 GPa. However, there are slight differences of E_z among different strain rates. The values of E_z at higher strain rates are generally higher than those at lower strain rates. However, those differences disappear when the data of Young's modulus are plotted against the orientation parameter $[P_2(\cos\theta)]$, shown in Figure 9. This implies that the mechanical properties of PET mainly depend on the molecular orientation, at least under the same temperature.

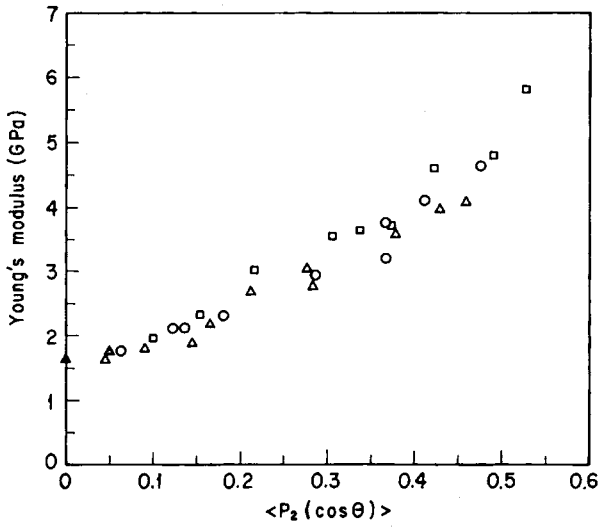

Figure 9 The Young's modulus (E_z) vs. $[P_2(\cos\theta)]$ at 80°C. (△) 0.0033 s^{-1}, (○) 0.01 s^{-1}, (□) 0.033 s^{-1}.

Figure 10 shows Young's modulus in directions with angles (θ) from the stretching direction. All curves show that modulus steadily rises from θ = 90°, which is the perpendicular direction, to θ = 0°, which is the stretching direction. The mechanical anisotropy becomes larger as the draw ratio increases. Comparing data at each angle, a modulus increase and decrease at θ = 0° and θ = 90° with draw ratio, respectively, is apparent. However, no specific trend can be found at other angles, which may result from the balance of E_z and E_x, where E_x is the modulus in the perpendicular direction.

Yield Stress

Figure 11 shows yield stress as a function of draw ratio at 0.001 s^{-1} and 80°C. The tendency of change of yield stress with extension ratio is found to be similar to that of Young's modulus. Yield stress increases with extension ratio from 5.3 MPa for isotropic PET to about 15 MPa at λ = 4.2. However,

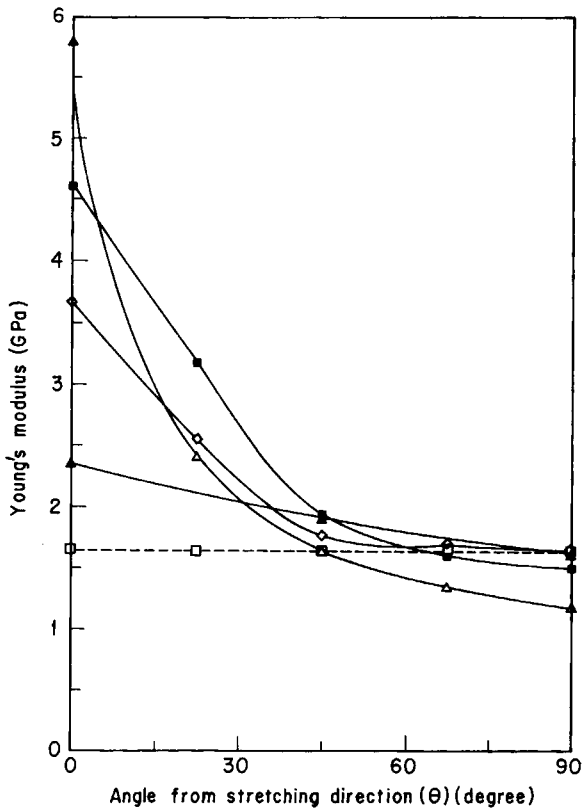

Figure 10 The Young's modulus at different angles from stretching direction vs. draw ratio. Oriented samples were prepared at 80°C and at 0.01 s^{-1}. (●) unstretched, (▲) λ = 2.35, (◇) λ = 3.35, (■) λ = 3.9, (△) λ = 4.4.

no obvious change can be observed for yield stress in the transverse direction.

Stress Ratio

There is an abrupt decrease of stress after the yield point, due to the occurrence of necking. The stress ratio, as defined above, could be an indication of the extent of necking and this value is calculated for a case at 0.01 s^{-1} and at 80°C, which is illustrated in Figure 12. The stress ratio before stretching is around 0.65. The stress ratio increases gradually, with draw ratio in the stretching direction, but it remain almost unchanged in the transverse direction.

CONCLUSIONS

This investigation revealed that the orientation parameter [$P_2(\cos\theta)$] of oriented PET varies strongly with both temperature and strain rate, but the strain-induced crystallinity seems dependent on temperature only. Therefore, the stretched PET samples, even with identical orientation, may have different morphological structures, which differences can be caused by the temperature used. As the orientation of extended PET increased, the mechanical properties in the stretching direction could be greatly enhanced, but those in the transverse direction remained unaltered or they declined slightly.

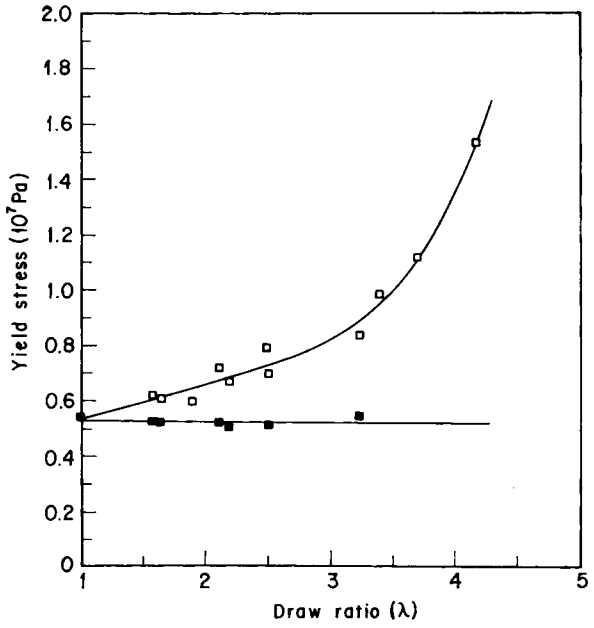

Figure 11 The yield stress vs. draw ratio. Oriented samples were prepared at 80°C and 0.01 s^{-1}. (□) experimental values along stretching direction, (■) experimental values perpendicular to stretching direction.

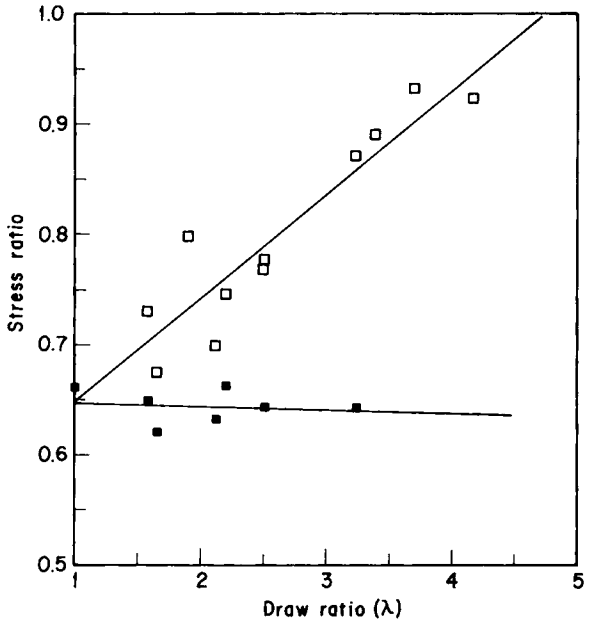

Figure 12 The stress ratio vs. the draw ratio. Oriented samples were prepared at 80°C and 0.01 s^{-1}. (□) experimental values along stretching direction, (■) experimental values perpendicular to stretching direction.

The authors would like to acknowledge with gratitude the financial support of the National Science Council, Taipei, Taiwan, Republic of China, through grant No. NSC 79-0405-E-002-11.

REFERENCES

1. G. Farrow and I. M. Ward, *Polymer*, **1**, 330 (1960).
2. S. R. Padibjo and I. M. Ward, *Polymer*, **24**, 1103–1112 (1983).
3. G. S. Y. Yeh and P. H. Geil, *J. Macromol. Sci. (Phys)*, **B1**(2), 251 (1967).
4. J. E. Spruiell, D. E. MacCord, and R. A. Beuerlein, *Trans. Soc. Rheol.*, **16**(3), 535 (1972).
5. I. M. Ward, *J. Polym. Sci. Polym. Symp.*, **58**, 1 (1977).
6. A. Misra and R. S. Stein, *J. Polym. Sci. Polym. Phys. Ed.*, **17**, 135 (1979).
7. J. W. Song and A. S. Abhiraman, *J. Appl. Polym. Sci.*, **27**, 1369 (1982).
8. T. Tareda, C. Sawatari, T. Chigono, and M. Matuso, *Macromolecules*, **15**, 988, 998 (1982).
9. D. I. Bower, K. K. P. Korybut-Daszkiewicz, and I. M. Ward, *J. Appl. Polym. Sci.*, **28**, 1195 (1983).
10. I. M. Ward, *Mechanical Properties of Solid Polymers*, 2nd Ed., Wiley, London, 1983, Chap. 10.

11. J. H. Nobbs, D. I. Bower, and I. M. Ward, *Polymer,* **17,** 25 (1976).
12. A. Cunningham, G. R. Daxies, and I. M. Ward, *Polymer,* **15,** 743, 749 (1974).
13. J. Purvis and D. I. Bower, *J. Polym. Sci. Polym. Phys. Ed.,* **14,** 1461 (1976).
14. J. H. Nobbs, D. I. Bower, and I. M. Ward, *Polymer,* **15,** 287 (1974).
15. K. J. Roe and W. R. Krigbaum, *J. Appl. Phys.,* **35**(7), 2215 (1964).
16. J. H. Nobbs, D. I. Bower, and I. M. Ward, *J. Polym. Sci. Polym. Phys. Ed.,* **17,** 259 (1979).
17. J. H. Nobbs and D. I. Bower, *Polymer,* **19,** 1100 (1978).
18. G. Bragato and G. Gianotti, *Eur. Polym. J.,* **19,** 803 (1983).
19. D. Goritz, F. H. Muller, and W. Sietz, *Progr. Colloid Polym. Sci.,* **62,** 114 (1983).
20. G. LeBourvellec, L. Monnerie, and J. P. Jarry, *Polymer,* **27,** 856 (1986).
21. J. Petermann and U. Rieck, *J. Polym. Sci. Polym. Phys. Ed.,* **25,** 279 (1987).
22. T. Thistletheaite, R. Jakeways, and I. M. Ward, *Polymer,* **29,** 61 (1988).
23. R. Ullman, *Macromolecules,* **11,** 987 (1978).
24. G. LeBourvellec, L. Monnerie, and J. P. Jarry, *Polymer,* **28,** 1712 (1987).

Received October 20, 1992
Accepted January 10, 1993